Comment on "Formation of Substorm Pi2: A coherent response to auroral streamers and currents" by Nishimura et al

Article

Published Version

Comment on "Formation of substorm Pi2: A coherent response to auroral streamers and currents" by Y. Nishimura et al.

I. Jonathan Rae,[1,2] Kyle R. Murphy,[1] David M. Miles,[1] Clare E. J. Watt,[1,3] and Ian R. Mann[1]

Received 11 December 2012; revised 9 May 2013; accepted 9 May 2013; published 25 June 2013.

Citation: Rae, I. J., K. R. Murphy, D. M. Miles, C. E. J. Watt, and I. R. Mann (2013), Comment on "Formation of substorm Pi2: A coherent response to auroral streamers and currents" by Y. Nishimura et al., *J. Geophys. Res. Space Physics*, *118*, 3488–3496, doi:10.1002/jgra.50336.

1. Introduction

[1] In their recent paper, *Nishimura et al*. [2012], hereafter termed N12, conclude that Pi2 magnetic field pulsations and auroral brightenings in the substorm expansion phase are driven coherently by flow bursts in the magnetotail. The authors claim not only that the flow bursts, auroral brightenings, and magnetic field perturbations all have periodicities in the Pi2 range but significantly also that the individual perturbations are all coherent and, as a consequence, infer a causal and one-to-one connection between them. In their scenario, fast earthward flows in the plasma sheet with fine structure in the Pi2 frequency range are responsible, in a piecewise and coherent fashion, for establishing one-by-one additional elements of the substorm current wedge (SCW) in response to each element of the flow burst fine structure. In other words, each subsequent flow burst adds an additional current element to the SCW, coherently driving both repeated enhancements in the aurora and step-like changes in the ground magnetic field across a wide longitudinal range such that "*each Pi2 pulse starts to rise simultaneously over a wide range of latitude from the auroral zone to the magnetic dip equator as well as over a wide longitudinal range*" [N12, abstract]. Each of these occurs at intervals separated by tens of seconds or minutes corresponding to the tail flow variations in the Pi2 band. The N12 claims are in stark contrast to the traditional explanation inferred from ground-based magnetic ULF wave observations that invokes bouncing Alfvén waves for the periodic structure of the Pi2s, and which necessarily includes propagation effects and precludes such large-scale coherence, based in part on the known fact that in order to establish a field-aligned current, one needs to send Alfvén waves along the field line [see, for example, *Olson*, 1999, and references therein].

[2] The conclusion reached in N12 that repeating flow bursts in the magnetotail directly drive auroral enhancements, related equatorward auroral streamers, and large-scale coherent Pi2 magnetic perturbation waveforms during substorm expansion phase onset relies on the predication that all auroral streamers are driven by fast flows in the magnetotail. There is, of course, evidence that some north-south aligned auroral streamers are connected to fast flows in the magnetotail [see, for example, *Zesta et al*., 2000]. A comprehensive examination of the mechanisms which link streamers to tail flow bursts was not addressed in N12, nor will it be addressed in this comment. Indeed, this comment is not concerned, and does not take issue, with the possible connection between tail flows and some N-S aligned arcs. However, it is the claimed coherency of the link between auroral streamers, the large-scale SCW, and global-scale coherent Pi2s which is advanced by N12 which we challenge here; the magnetotail drivers of auroral streamers themselves are not the focus of this comment nor were they the focus of N12.

[3] The proposed coherence and causal hypothesis in N12 rests upon three logical assertions.

[4] 1. Expansion phase intensifications along the poleward boundary of the aurora are repetitive, and each intensification leads to an equatorward propagating auroral streamer.

[5] 2. There is a one-to-one correspondence between each individual expansion phase auroral intensification and each individual magnetic pulsation.

[6] 3. Each magnetic pulsation is coherent across all latitudes for the duration of the period of the formation of the substorm current wedge.

[7] The observational evidence presented in N12 claims to address these three assertions, which are at the core of their hypothesis coherently linking periodic flow bursts to Pi2s waveforms, through a multi-instrument study. The analysis includes observations of auroral brightness from the Time History of Events and Macroscale Interactions during Substorms (THEMIS) all-sky imagers (ASIs) [*Mende et al*., 2008] and magnetic field perturbations from multiple arrays of ground-based magnetometers (from Canadian Array for Realtime Investigations of Magnetic Activity (CARISMA) [*Mann et al*., 2008] and THEMIS ground-based magnetometers [*Russell et al*., 2008; *Peticolas et al*., 2008]) in addition to those from the Canadian Magnetic Observatory System (http://geomag.nrcan.gc.ca/obs/canmos-eng.php), Athabasca University THEMIS UCLA Magnetometer Network (http://autumn.athabascau.ca), and Geophysical Institute Magnetometer

Additional supporting information may be found in the online version of this article.

[1]Department of Physics, University of Alberta, Edmonton, Alberta, Canada.

[2]Now at Mullard Space Science Laboratory, University College London, Holmbury St. Mary, Dorking, Surrey, UK.

[3]Now at Department of Meteorology, University of Reading, Earley Gate, Reading, UK.

Corresponding author: I. J. Rae, Mullard Space Science Laboratory, University College London, Dorking RH5 6NT, UK. (jonathan.rae@ucl.ac.uk)

2169-9380/13/10.1002/jgra.50336

Array (http://www.asf.alaska.edu/program/gdc/project/magnetometer) magnetometer arrays. In this comment, we reanalyze the data sets presented in N12 and demonstrate that the ground-based magnetic field and auroral observations do not support the conclusion that repetitive fast flows in the magnetotail coherently and directly drive step-like increases in the SCW in a piecewise fashion.

2. Auroral Intensifications: THEMIS All-Sky Imager Analysis

[8] In N12, a new type of keogram is introduced that aims to highlight quasiperiodic activations of the aurora. A traditional keogram takes one north-south slice through the aurora to provide information on the structure of the aurora in one meridian and its poleward or equatorward motion, whether it is formed using data from a meridian scanning photometer or from a section of an ASI image. The new type of keogram used in the data presentation in N12 displays the highest intensity at each latitude from any longitude in the ASI field of view (FOV) as a function of time. In this way, it is hoped that the structure of the rapidly evolving active aurora can be captured in a reduced format. With such an approach, the authors of N12 seek to minimize the effects of any longitudinal motion of auroral forms within the ASI FOV—especially those which move the brightest arc activity and motion out of the single meridian of the traditional keogram. The implicit assumption underpinning the interpretation of this alternative keogram is that the auroral features under study are aligned in the east-west direction and are the brightest features in the ASI FOV. This will likely be true in the growth phase of a substorm but will be a poor representation of auroral morphology during dynamic times such as those in the substorm expansion phase which are the focus of the studies in N12 (see the supporting information, particularly Movies S1 and S2). To make the necessary clear distinction between a traditional keogram and the new analysis technique introduced in N12, we refer to this analysis as an "auroral maxogram."

[9] In order to reproduce the auroral maxograms as shown in N12, certain assumptions about their analysis must be made. The maxograms displayed in Figures 2, 4, 6, and 7 of N12 discard entire meridians of ASI data if any portion is obviously contaminated by the Moon, or its reflection (Y. Nishimura, personal communication, 2012). Figures 1a–1e show an auroral maxogram using the N12 approach described above, the time evolution of the longitudes of the maximum intensities observed at each latitude (color coded), and three ASI images at times corresponding to auroral intensifications identified by the yellow arrows in N12's Figure 3. Overplotted on each ASI image in Figure 1 are color-coded circles marking the geomagnetic longitude of those ASI pixels that are used to construct the maxogram. Plots for each identified streamer identified in N12's Figure 3 are included as Figure S1 in the supporting information. Subtle differences exist between the maxogram in Figure 1a and N12's Figure 2h, e.g., a ~1° offset in latitude between some auroral features and an assumed linear color scale of 1000–15,000 counts. Nevertheless, Figure 1a remains a good facsimile of Figure 2h in N12, reproducing all salient auroral features.

[10] From the combination of the ASI images and the maxograms in Figure 1, it is clear that what appears as a single auroral feature in a maxogram is not, in fact, constructed from a contiguous single auroral form in the ASI image. The ASI snapshots in Figures 1c–1e demonstrate clearly that the intensity as a function of latitude is constructed from a number of discrete and apparently optically unconnected auroral forms that are from very different longitudes and contain rapidly varying auroral intensities (see Movie S1 in the supporting information). Each pixel in the two-dimensional maxogram is independent from any other pixel and is frequently drawn from different auroral features which can be very far from, and certainly not contiguous with, its direct neighbors. Figure 1b shows the temporal evolution of pixel location in the maxogram. The longitudinal locations of the maximum intensities show no trends in the location of pixels as a function of time; indeed, the location of each pixel used to construct the maxogram varies unpredictably over the entire ~9° longitude used in the construction of N12's Figure 2. Importantly, for the interpretation of enhancements in the maxogram, we mark the location of auroral streamers identified in N12 using yellow arrows in Figures 1c–1e. There are very few pixels related to auroral streamers that are picked out in the maxogram: At 08:39:48 UT (Figure 1c), three pixels between 69.5 and 70.5° are identified; at 08:37:18 UT (Figure 1d), there are four identified points at lower latitudes (~68.5–69.5°); and at 08:43:00 UT (Figure 1e), only high-latitude elements of the auroral streamer are identified in the maxogram. It can be seen from Figures 1c–1e that the maxogram analysis often triggers on the residual light contamination from the Moon or from stars, potentially masking otherwise important auroral features. Figures 1c–1e demonstrate that maxogram intensity pixels are often selected in a meridian corresponding to the eastern boundary of the Moon removal. More data snapshots are shown in Movies S1 and S2, where this artifact is clearly seen.

[11] In summary, the maxogram technique as presented by N12 and as reproduced in this comment conflates auroral features widely separated by latitude and longitude with phenomena such as stars and the residual halo from the Moon. The maxogram creates seemingly coherent brightness enhancements which, instead of being a good representation of auroral morphology, are simply an artifact of the data analysis used to create the maxogram. Put simply, rather than providing a useful tool for examining the dynamics of contiguous and spatially connected auroral forms that display variations in auroral intensity, the maxogram technique fails to capture or represent the salient dynamic aurora.

[12] When combining observations from auroral cameras and ground-based magnetometers, it is important to note that the magnetometer integrates the effects of all currents in the overhead ionosphere according to the Biot-Savart law. If the auroral forms measured by the camera are indicators of the current systems present in the ionosphere, then a subset of the ASI data (i.e., those data used to create Figure 1a) necessarily only describes a subset of current systems in the region. Regardless of the problems listed above, in this comment, we also investigate whether it is possible to use the maxogram analysis to generate a simplified but nonetheless meaningful summary of the local auroral activity, and hence the local current systems, in order for it to represent a meaningful data product which can be compared to information derived from ground-based magnetometer data. In the next section, we show a maxogram generated using a second approach that includes all auroral information from one

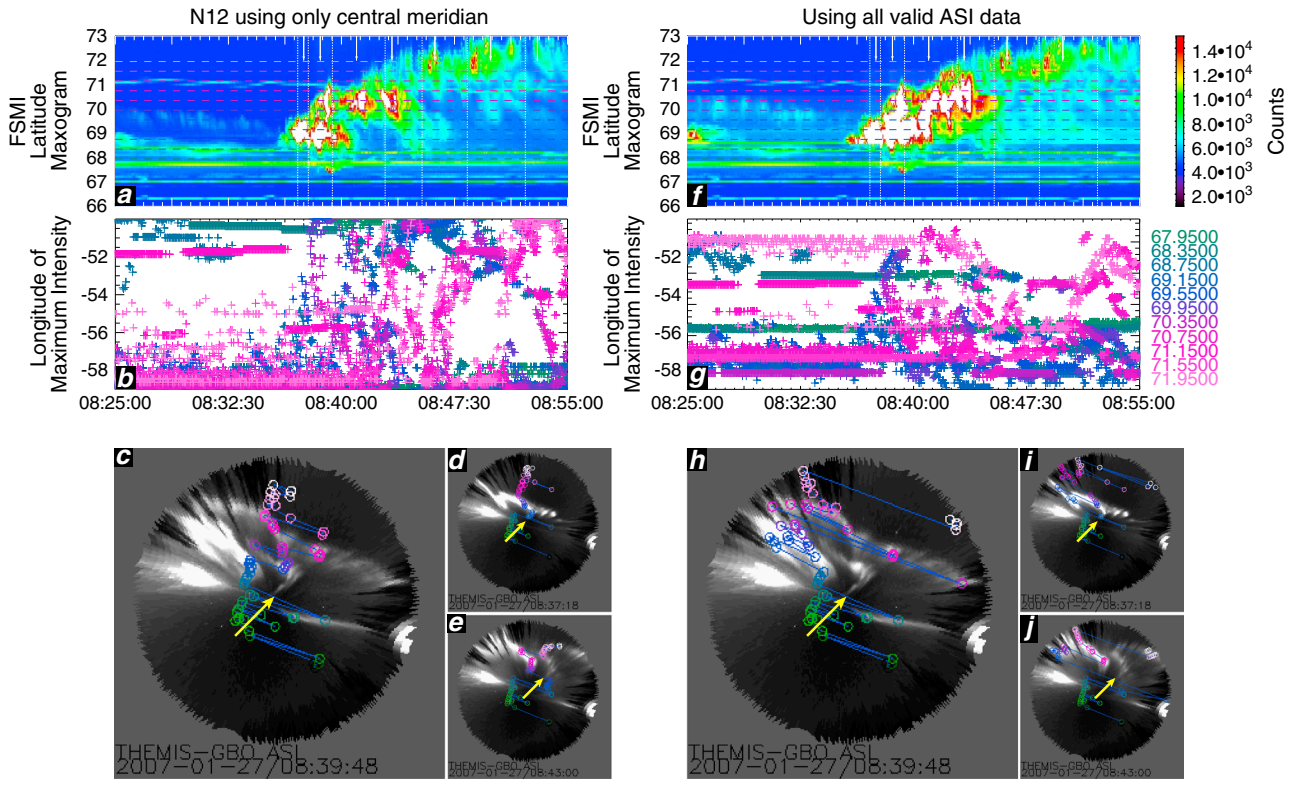

Figure 1. Auroral maxogram analysis of (a–e) the meridians uncontaminated by moonglow, and equivalent to those presented in N12, and (f–j) the maxograms including all latitudes and longitudes that are uncontaminated by moonglow. Figures 1a and 1f show auroral maxograms from the THEMIS FSMI ASI, Figures 1b and 1g the longitudinal locations of the pixel of maximum brightness as a function of latitude and time, and Figures 1c–1e and 1h–1j three times asserted by N12 to represent auroral streamers captured by the maxogram analysis and be correlated with ULF pulsations. Additional times are shown in Figure S1. The dashed white lines and the arrows in Figures 1a and 1f are the times and intervals marked to be significant by N12 in their Figure 2.

THEMIS ASI that is more likely to include all contributing auroral features.

[13] Figure 1f shows a maxogram generated using this second approach, where all valid THEMIS ASI data from the same camera as in Figures 1a–1e are analyzed, but this time where only those *pixels* obviously contaminated by moonglow are removed. Using a similar color scale to Figure 1a, the significant thing to note is that the recurring enhancements of auroral intensity which were at the core of the conclusions drawn in N12 are no longer seen in our alternative maxogram (Figure 1f). During the active period following onset, Figure 1g demonstrates that the longitude of the maximum intensity at each latitude is now even more variable, ranging from −45° to −65° in short and dynamic periods (see Movies S1 and S2 in the supporting information). Comparison of Figures 1c–1e and 1h–1j demonstrates even more challenges for the validity of the maxogram approach since different auroral forms are selected in each version of the analysis. Additionally, the largest values of auroral brightness often occur in meridians outside of the data subset used in N12 to create the maxogram in their Figure 2. Neither maxogram algorithm reliably selects pixels from auroral streamers (cf. one pixel of an auroral streamer in Figure 1i). Overall, the maxogram presented in N12's Figure 2 emphasizes auroral features which may not necessarily correspond to the brightest aurora in the frame and rarely correspond to the auroral streamers which it was designed to characterize. There is no direct link between features in the maxogram and specific auroral forms. Hence, we show that although the aim of the maxogram is to capture the motion of the aurora in a simpler format than a time series of 2-D images, this analysis technique does not do so. As we also show in Figures 1a and 1f, the maxogram analysis also neglects other auroral forms that will contribute to the magnetic field perturbations and which are important elements of the overall auroral dynamics.

3. Coherence of Aurora and Waves

[14] The inferred correlation between auroral intensity and Pi2 ULF wave activity presented in N12 is derived solely on the basis of a visual inspection of the data. No quantitative method is described that correlates auroral intensifications and ULF pulsations in the magnetometer data. In Figure 2, we demonstrate how the choice of both color scale and subsection of an ASI field of view affects the conclusions drawn in N12. Figures 2a and 2b show the reduced FOV that N12 use in two different color scales, where entire meridians with obvious Moon contamination are omitted. Figure 2c shows the same color scale as N12 and Figure 2b but omits only pixels contaminated by obvious moonglow, rather than entire meridians. Also plotted are N12's auroral streamer (arrows) and low-latitude ULF wave minima (dashed lines).

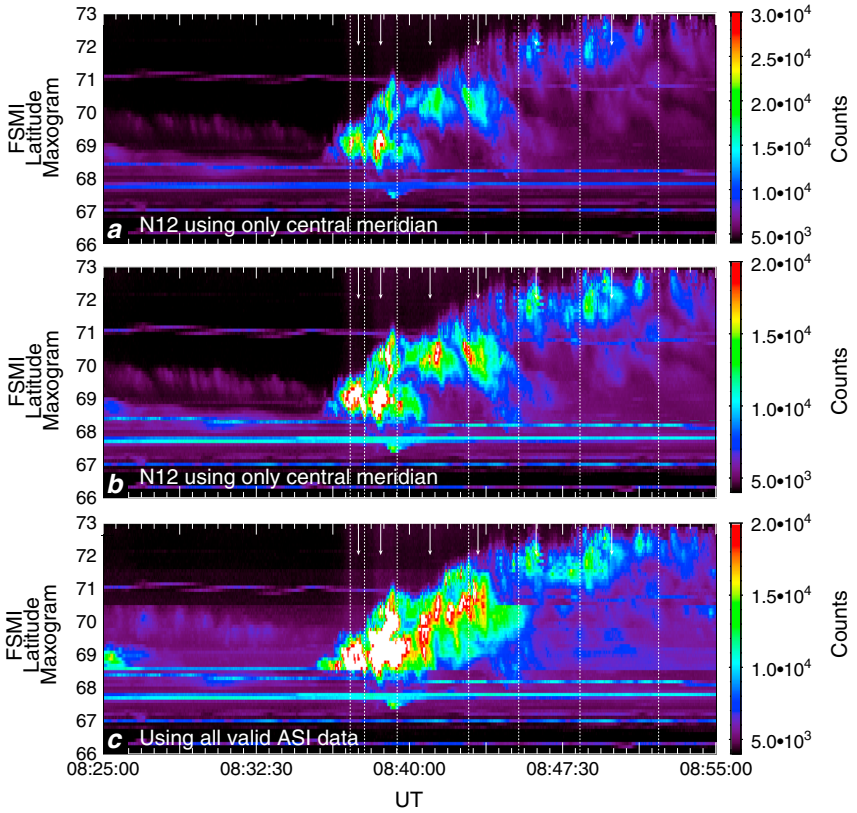

Figure 2. A demonstrated example of how the choice of color scale and subsection of field of view affects the conclusions drawn. The same subset of data used in N12 is shown with (a) an alternate color scale and (b) the same color scale as N12, where entire *meridians* with obvious Moon contamination are omitted. (c) The same color scale as N12 and Figure 2b but constructed using all *pixels* that do not contain obvious moonglow. Overplotted on all panels of Figure 2 are arrows that correspond to auroral streamer times as identified in N12. The white dashed lines denote ULF wave minima, presumably identified in N12 from low-latitude ground-based magnetometer stations. Note the differing auroral forms that are shown in each color scale and in each analysis technique.

[15] Briefly, there is no specific reason to consider either Figure 2a or 2b to be more or less physically motivated, but each leads to different "by eye" interpretation of the observations, as evidenced by the apparent different number of auroral intensifications seen in both panels. Figure 2a shows anywhere between one and four auroral intensifications between ULF wave minima, Figure 2b showing even more. Figure 2c is even more interesting and complex. Indeed, it is difficult to visually determine how many activations are seen using the entire ASI FOV, but we simply direct the reader to the ULF wave period encompassing the third white arrow (08:39:30–08:43:00 UT) period, during which one ULF wave cycle encompasses upward of six auroral forms. We are thus forced to ask the following questions.

[16] 1. Why do N12 eschew five other equally intense auroral activations in favor of one specific auroral activation in the middle of this period?

[17] 2. Why is this specific auroral form responsible for enhancing the SCW, i.e., the ULF wave signature, as opposed to any of the other equally intense five auroral features?

[18] What is clear is that there is no one-to-one relationship between one specific ULF wave cycle and a coherent auroral form. We also note that there is no one-to-one relationship between the "center" of each maxogram enhancement identified by N12 and the magnetic field minima, even in the data as presented in N12. Enhancements occur variously in the beginning, middle, and end of the presented ULF wave cycles as well as at the border between cycles, leading the reader to question the original N12 conclusions even before considering all the ASI data.

[19] Our reanalysis of N12 in sections 2 and 3 (Figures 1 and 2) shows clearly that the identified streamers are not even the dominant, and certainly not the brightest, auroral features in the maxograms, in the entire ASI FOV, or, indeed, in the substorm expansion phase. Therefore, even in the absence of evidence for a robust coherence with the magnetic data, we are left wondering why so much importance is attached to the small-scale and optically dim auroral streamers within the much brighter auroral surge. Considering the full, complex optical structure of the auroral surge, it is not expected that the global ionospheric magnetic ULF wave response would preferentially pick out the streamers as a coherent driver—rather than, say, responding to the processes linked to and driving all of the other brighter and very structured complex optical features in the surge. Below, we discuss this ULF response.

4. A Coherent ULF Wave Response?

[20] The conclusions of N12 about the coherence of the tail flow-aurora-Pi2 response also rely on a claimed coherence of Pi2 pulsations across a large range of latitudes (and longitudes) during substorm expansion phase onset. The extensive combined North American ground-based magnetometer data set can reveal much about the ionospheric current systems during onset. In interpreting ground-based magnetic observations, it is important that all available data should be included in the analysis and that the same coordinate systems are employed so that comparisons between different stations are accurate and reliable. The interpretation of correlations between two magnetometer time series during substorm expansion phase onset is not straightforward, since there can be multiple contributions to the magnetic field perturbations even within any specific frequency band from different sources (e.g., from both magnetic bays and pulsations). We expand on these points below.

[21] In Figure 2 of N12, where Pi2 waveforms from a range of magnetometer stations are compared, a mix of geodetic and geomagnetic coordinate systems is used in the data presentation. Both the amplitude and the phase of a ULF wave can be dependent upon the coordinate system in which the data are presented. The difference between geodetic and geomagnetic coordinate systems at Fort Smith (FSMI) and Yellowknife (YKC), for example, is a rotation about the Z axis of 22.77° and 20.12°, respectively. In our reanalysis of the ground-based magnetometer data presented in N12, we use a consistent geomagnetic coordinate system to study the relative phases of ULF pulsations during the first event of N12.

[22] Figure 3 shows a series of panels of magnetometer data that lie approximately along one meridian, for comparison with the station locations highlighted in N12's Figure 1, but of which only a subset of these available stations was presented in N12's Figure 2. All available magnetometer stations in the relevant meridian are included in our Figure 3, from high latitude (top) to low latitude (bottom); those omitted from Figure 2 of N12 are indicated in red. Note that Figures 3b and 3l show data from the FSMI magnetometer station that is colocated with the ASI used in N12's Figure 2h. This station is omitted from the analysis in N12. The left column (Figures 3a–3j) shows the H component, and the right column (Figures 3k–3t) shows the 40–300 s period filtered ULF wave data. Overplotted on Figure 3 are dashed lines which correspond to the low-latitude amplitude minima as shown in N12's Figure 2g. Note that these lines range between 140 and 230 s apart and so are outside of the 40–150 s Pi2 period band [*Jacobs et al*., 1964] and the "40–150 s passband" described in N12's Figure 2g. It is unclear therefore as to whether the low-latitude magnetic field data shown in N12's Figure 2 are mislabeled as "40–150 s passband" or whether the ULF minima are an artifact of the analysis. What is clear is that the waves studied in N12's Figure 2 are outside the Pi2 period band and that the N12 analysis depends fundamentally on an extensive analysis of waves which, by their own description, their filters reject. We will therefore refer to these waves as ULF waves and show filtered data in the 40–300 s period band that encompasses both Pi2 periods and the pulsation periods highlighted in N12.

[23] Figures 3k–3t show clearly that the relative phase across magnetometers is neither preserved and constant across all latitudes, as claimed by N12, nor maintained for an extended period of time. From a visual inspection, the lower latitude stations (Red Deer (REDR) and Carson City (CCNV)) appear essentially in phase during the interval, where magnetic minima coincide with the dashed vertical lines as shown in N12. At higher latitudes, however, there is no consistent relationship between the minima of the pulsations in Figure 3 and the location of the dashed lines from N12. Depending on the latitude, in the same time period, the dashed lines from N12 can correspond to ULF wave minima, maxima, or points in between. The frequency content of the high-latitude time series is also more complicated than that of the low-latitude time series. Overall, the (40–300 s period) filtered data from all the available magnetometer stations do not demonstrate a coherent ULF wave response—and the N12 conclusion that flow bursts in the tail create a latitudinally coherent signal is not validated once the data are more completely analyzed.

[24] Note that it is well known that wave propagation from the magnetosphere to the ionosphere, for example, in response to flow bursts or other drivers, can have a complex structure both in frequency and in latitude-dependent phase. Time-of-flight considerations [e.g., *Chi et al*., 2001], the possible excitation of field line resonances [e.g., *Takahashi et al*., 1988; *Keiling et al.*, 2003; *Rae et al*., 2007], and the influence of the local Alfvén frequency on a given field line at a given latitude [e.g., *Menk et al*., 1999] can all impact the amplitude and phase of the pulsations on the ground. However, in N12, it is asserted not only that Pi2 waves simply adopt the same frequency as the putative flow bursts responsible for the auroral streamers but that the response across latitude and longitude is coherent. Furthermore, during substorm expansion phase onset, the field line topology is likely rapidly evolving, particle injections may alter the density and hence Alfvén continuum, and time-of-flight considerations will hence likely not be constant throughout the period of the duration of the formation of the SCW. Overall, given these considerations, it would not be expected that the phase of Pi2 pulsations across all latitudes would be constant—and the more detailed analysis presented here shows that this is clearly not the case. The specifics of the relationship between Pi2 pulsations and fast flows in the magnetotail have been expounded at length by *Kepko and Kivelson* [1999] and *Murphy et al*. [2011] and reviewed extensively by *Keiling and Takahashi* [2011], demonstrating a clear latitudinal dependence of both ULF wave amplitude and phase to periodic fast flows in the magnetotail. Indeed, we demonstrate in Figure 3 that there is no constant phase between Pi2 pulsations when data from all available stations are taken into account.

[25] Correlation is often used to examine the coherence of two wave signals. The inset in N12's Figure 2n is used as quantitative evidence of the correlation (and coherence) between the middle- and low-latitude magnetometer data, some ~20° apart. The geodetic X component of Ministik Lake (MSTK) is correlated with the geomagnetic H component of CCNV. This panel is the only correlation presented for this interval in N12 and maximizes at $R > 0.9$ (equivalent to $R^2 \sim 0.8$) at close to zero lag. Leaving aside the incompatible

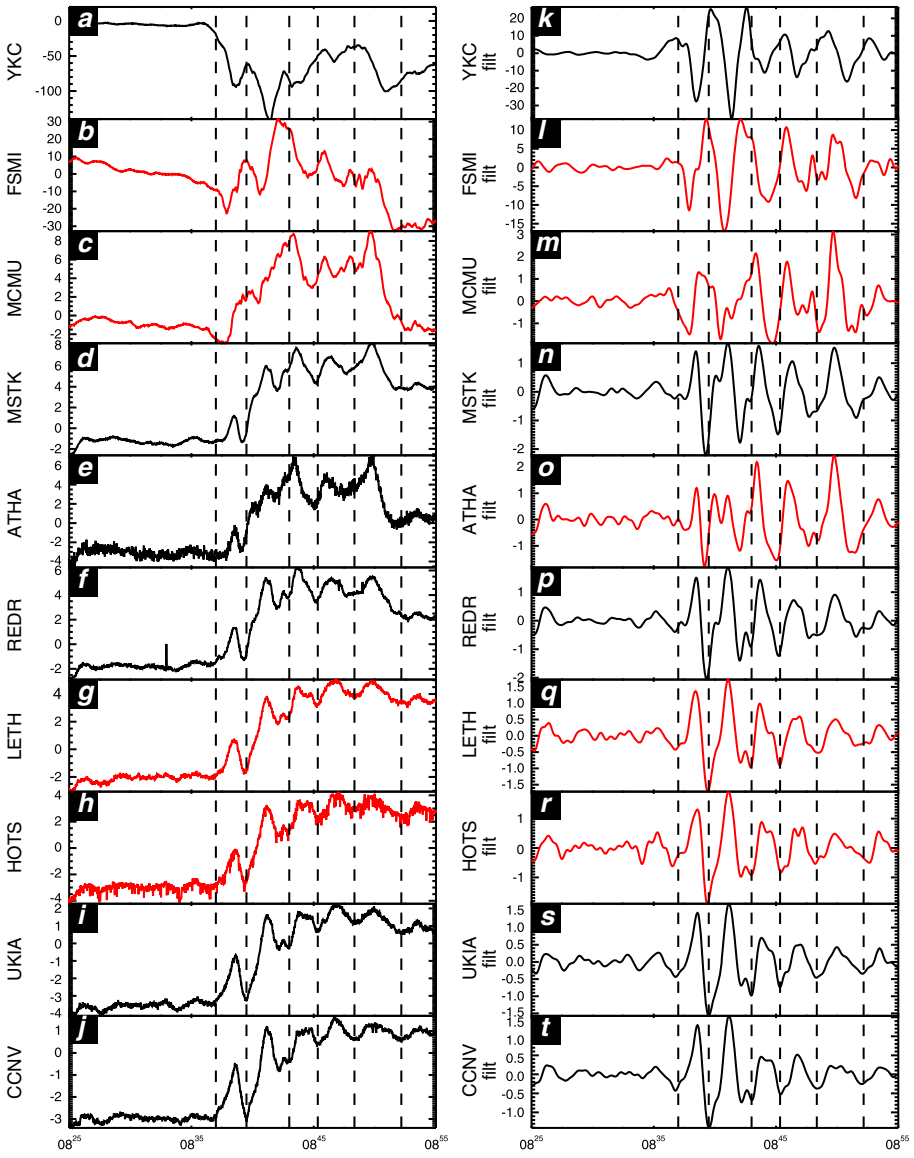

Figure 3. (a–j) The H component (geomagnetic north-south) magnetic field data from a quasi-latitudinal cut through the entire set of magnetometers available, of which the locations are shown in N12's Figure 1 but of which a subset of these data is shown in N12's Figure 2. Plotted in Figure 3 are the ULF wave pulsations appealed to in N12 as Pi2 waves which are, in fact, >200 s period. (k–t) The 40–300 s period filtered time series from the raw H component data shown in Figures 3a–3j. Overplotted on Figure 3 are the locations of times identified in N12 to be significant.

coordinate systems used in N12, we proceed to reinvestigate this correlation and its cause.

[26] The magnetometer time series recorded during expansion phase onset are typically considered to predominantly comprise a combination of a low-frequency large magnetic bay and higher-frequency ULF perturbations [*McPherron et al.*, 1973]. In order to examine the source of the correlation presented by N12 as evidence in support of their conclusion, we derive a toy model of a substorm time series and examine the correlations between its bay and ULF wave components. We then return to a correlative analysis based on observed magnetometer data used in N12. Figure 4 shows the correlation analysis of (left) a pair of simulated substorm magnetometer time series and (right) a pair of observed magnetometer time series (from the MSTK and CCNV stations, used in N12's Figure 2n). We simulate two idealized magnetometer responses to substorm onset using a step function, a single sinusoidal ULF wave, and some low-amplitude uncorrelated noise. One of the simulated time series contains a ULF wave with 66 s period; the other has a 75 s period ULF wave. The combined time series are shown in Figure 4a, the ULF waves in the simulated signals are isolated in Figure 4b, the step function plus the noise is isolated in Figure 4c, and the noise is shown in Figure 4d. The linear Pearson correlation coefficients for each pair of time series are indicated in each panel. By comparing the isolated idealized signals, we

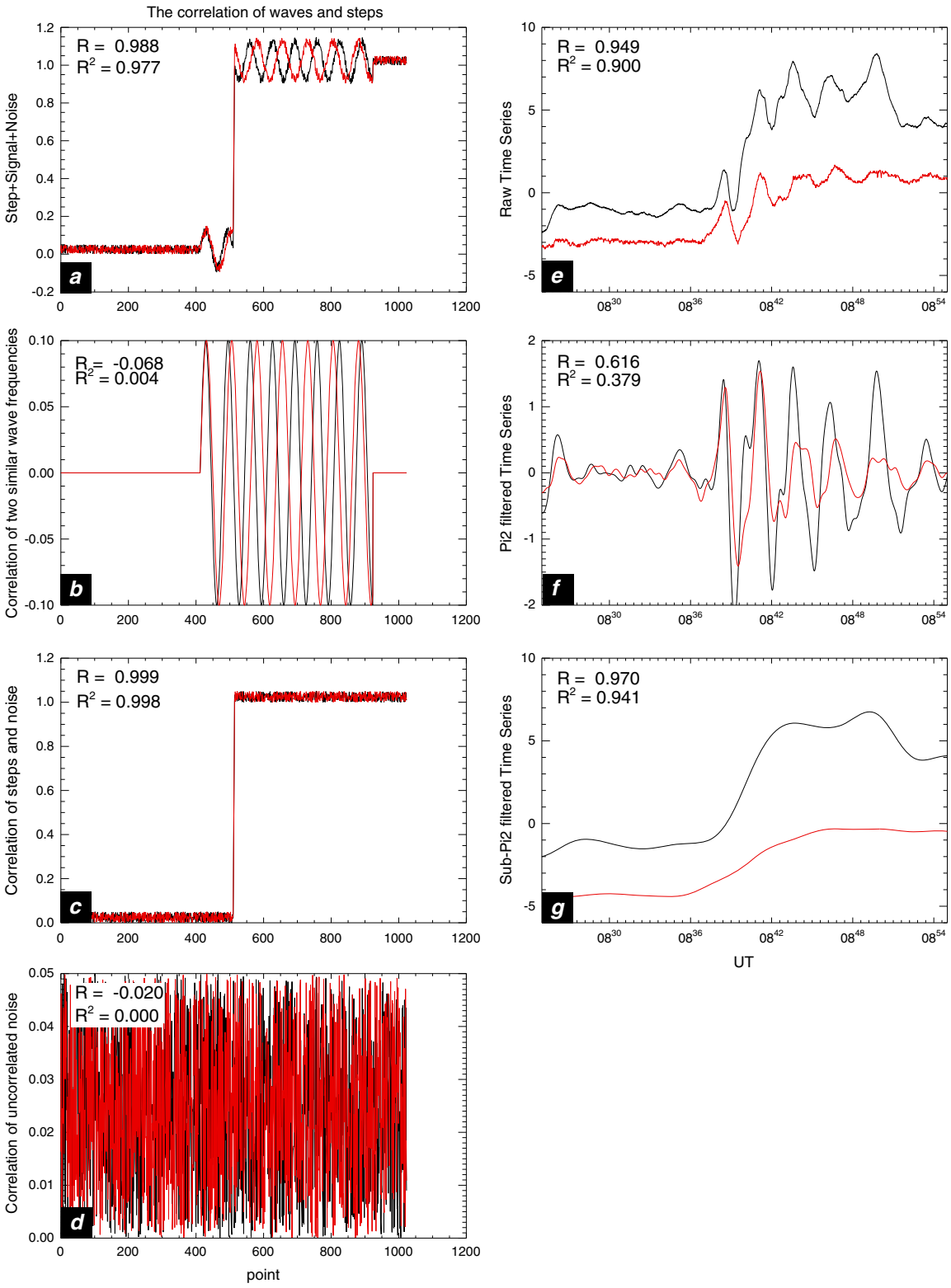

Figure 4. Simulated and real data used to demonstrate the lack of coherence between ULF waves observed at two stations shown in N12's Figure 1. (a–d) A simulated series of signals with waves of 66 s period (red) and 75 s period (black) superposed upon a step function with uncorrelated low-amplitude noise, the simulated waves, the step function with uncorrelated noise, and, finally, the uncorrelated noise time series, respectively. (e–g) The two time series from N12's Figure 2 (inset) from MSTK and CCNV, the 40–300 s period filtered time series for reasons stated in the text, and the >300 s period component of the time series, which is primarily the low-frequency trend of the time series throughout the interval, respectively. On each panel is the unsquared and squared linear correlation coefficients used in N12 to demonstrate that the ULF waves are "coherent" across all latitudes.

can determine that the majority of the correlation in Figure 4a is controlled by the near-perfect linear correlation of the large-scale step functions shown in Figure 4c. Moving to the observed magnetometer time series, which cannot be so cleanly separated into constituent parts, Figure 4e shows the two time series of H component MSTK and H component CCNV, Figure 4f the ULF wave (40–300 s period) filtered time series, and Figure 4g the >300 s period component of the time series. Again, all the correlation coefficients for each pair of time series are indicated in each panel. The correlation ($R = 0.970$, $R^2 = 0.941$) of the long-period signals (the magnetic bays) in Figure 4g is significantly higher than the correlation ($R = 0.616$, $R^2 = 0.379$) of the filtered ULF wave signals (Figure 4f). Hence, 94% of the magnetic bay of one magnetometer time series can be reproduced from the other time series, whereas only 38% of a ULF wave time series can be recreated from the other ULF wave time series. We conclude that the large correlation between MSTK and CCNV ($R = 0.949$, $R^2 = 0.900$) primarily arises from the low-frequency trend (or magnetic bays) as opposed to any similarity between the ULF waves observed at the two different magnetometer stations. The high correlation of magnetic bay signals is a well-established low-middle latitude indication of the presence of the SCW at higher latitudes [*McPherron et al*., 1973]. As we also show, the ULF waves that occur at auroral latitudes during substorm onset are not typically coherent, are not linearly well correlated (with zero lag), and hence cannot be considered to be coherent.

[27] We must reiterate that a visual inspection of magnetometer time series cannot assert the coherence of ULF waves, because the time series are a complicated superposition of magnetic perturbations with different periods and from different sources. Since the discovery that the evolution of the intensity of the optical auroral emissions during substorm onset is strongly tied to the growth of ULF wave amplitudes, tools have been developed in order to study the spectral properties of electromagnetic wave activity [e.g., *Samson and Olson*, 1980; *Nosé et al*., 1998; *Milling et al*., 2008; *Plaschke et al*., 2008; *Murphy et al*., 2009; *Rae et al*., 2009; *Kataoka et al*., 2009; *Rae et al*., 2012]. Such analysis tools would provide a significantly better approach to characterize any potential link between Pi2 waveforms and auroral emissions than the approach used in N12.

5. Summary

[28] In N12, it is argued that recurring flow bursts in the magnetotail directly drive intensifications of the aurora during the substorm expansion phase and that these auroral intensifications are responsible for coherently driving magnetic ULF pulsations as observed over large longitudinal and latitudinal scales by ground-based magnetometers. Specifically, it is claimed in N12 that "*expansion-phase intensifications near the poleward edge of the auroral bulge occur quasiperiodically with one-to-one correspondence to Pi2 pulses*" and further concluded that "*substorm Pi2s are driven by multiple plasma sheet flow bursts, each driving a Pi2 pulse*." These conclusions rely upon the reliable identification of every intensification at the poleward boundary of the auroral bulge, their correlation with low-frequency ground-based magnetometer ULF perturbations, and the coherence of the magnetometer perturbations over a wide range of latitudes. Our reanalysis of one of the events presented in N12 demonstrates the following.

[29] 1. *Auroral intensifications*. We demonstrate that the use of maxograms (where the maximum auroral intensity at any longitude with an ASI FOV is used to create a keogram) for the presentation of auroral data in N12 does not provide a reliable basis for assessing periodic streamer features in the ASI data. For the case we reanalyzed, the maxograms do not capture coherent auroral forms, do not reliably capture the brightest local aurora, and do not contain any features which characterize the auroral streamers. Conclusions drawn from the maxograms can also be biased heavily by data selection and color scale. Overall, the periodicities of the streamers identified using maxograms in N12 are not reliable.

[30] 2. *Coherence of aurora and waves*. In this comment, we demonstrate that there is no clear and consistent phase relationship between maximum auroral brightness and ground-based magnetic wave signals across the large latitudinal and longitudinal extent claimed by N12. The implied coherence of ULF waves and auroral intensities was based solely upon a visual inspection of the maxogram and selected ULF wave time series in N12; however, we have demonstrated that the N12 results are biased through data selection and color scale. Furthermore, the auroral streamers that are postulated in N12 as the drivers of ULF pulsations are but one small, dim part of a complex, bright auroral display; indeed, the streamers are not even well represented in the maxograms which are used by N12 to characterize them. From a physical perspective, it is not clear why a ground magnetometer should respond solely, preferentially, and coherently to this minor feature in the aurora. Indeed, more detailed analysis of the data shows that the magnetic response is, in fact, far from coherent and better explained by more standard Alfvén wave propagation models than the direct coherent driving postulated in N12.

[31] 3. *A coherent ULF wave response*. We demonstrate that contrary to the conclusions in N12, the magnetometer ULF perturbations are not coherent across the nightside ionosphere. Specifically, the data do not support the N12 conclusion that "*each Pi2 pulse starts to rise simultaneously over a wide range of latitude from the auroral zone to the magnetic dip equator as well as over a wide longitudinal range*" [N12, abstract]. The quantitative coherence between ULF waves which N12 claim is shown for their first event is also shown here to be due to the similarity in magnetic bay signatures associated with substorm expansion phase onset, rather than due to any true correlation between the waves. Consequently, we assert that the correlation presented by N12 does not represent evidence in support of their conclusion of a large-scale coherent ULF wave response.

[32] Works spanning four decades [e.g., *Rostoker et al*., 1975; *Gelpi et al*., 1987; *Murphy et al*., 2012] have shown that the SCW is composed of a number of upward and downward field-aligned current (FAC) elements that, only when averaged, reduce to the traditional *McPherron et al*. [1973] view of a downward current post-midnight and an upward current pre-midnight. In short, the SCW houses far more complex current systems than proposed in N12. If multiple, simultaneous tail flows are responsible for this long-established complex structure, then only some of these flows have an optical signature and only some of these flows have a magnetic signature. This is incompatible with the one-to-one paradigm suggested in N12.

[33] In summary, the analysis presented in N12 contains several fundamental errors and encompasses several erroneous implicit assumptions that mean no conclusion can be reached regarding the development and dynamics of the coupled magnetotail-aurora system during the substorm expansion phase. The concept of a global, coherent, directly driven one-to-one relationship between tail flow bursts, auroral streamers, Pi2s, and the substorm current wedge described in N12 is not supported by the data and, in our opinion, is an overly simplistic and inaccurate representation of the substorm expansion phase dynamics.

[34] **Acknowledgments.** I.J.R. and C.E.J.W. are funded by the Canadian Space Agency. K.R.M. is funded by Alberta Innovates. I.R.M. is supported by a Discovery grant from Canadian NSERC. CARISMA is operated by the University of Alberta and funded by the Canadian Space Agency. We acknowledge NASA contract NAS5-02099 and V. Angelopoulos for the use of data from the THEMIS mission. The ground-based component of the THEMIS mission is funded by NSF award 1004736. We thank S. Mende and E. Donovan for the use of the THEMIS ASI data; the CSA for the logistical support in fielding and data retrieval from the GBO stations; S. Mende and C. T. Russell for the use of the GMAG data; Martin Connors and C. T. Russell for the use of the AUTUMN data; and the Canadian Magnetic Observatory Network (CANMON), maintained and operated by the Geological Survey of Canada, for providing the data used in this study (http://www.geomag.nrcan.gc.ca).

[35] Robert Lysak thanks the reviewers for their assistance in evaluating this paper.

References

Beamish, D., H. Hanson, and D. Webb (1979), Complex demodulation applied to Pi2 geomagnetic-pulsations, *Geophys. J. R. Astron. Soc.*, *58*, 471–493, doi:10.1111/j.1365-246X.1979.tb01035.x.

Chi, P. J., et al. (2001), Propagation of the preliminary reverse impulse of sudden commencements to low latitudes, *J. Geophys. Res.*, *106*, 18857–18864.

Gelpi, C., H. J. Singer, and W. J. Hughes (1987), A comparison of magnetic signatures and DMSP auroral images at substorm onset: Three case studies, *J. Geophys. Res.*, *92*, 2447–2460, doi:10.1029/JA092iA03p02447.

Jacobs, J. A., Y. Kato, S. Matsushita, and V. A. Troitskaya (1964), Classification of geomagnetic micropulsations, *J. Geophys. Res.*, *69*, 180.

Kataoka, R., Y. Miyoshi, and A. Morioka (2009), Hilbert-Huang transform of geomagnetic pulsations at auroral expansion onset, *J. Geophys. Res.*, *114*, A09202, doi:10.1029/2009JA014214.

Keiling, A., and K. Takahashi (2011), Review of Pi2 models, *Space Sci. Rev.*, *161*, 63–148, doi:10.1007/s11214-011-9818-4.

Keiling, A., K.-H. Kim, J. R. Wygant, C. Cattell, C. T. Russell, and C. A. Kletzing (2003), Electrodynamics of a substorm-related field line resonance observed by the Polar satellite in comparison with ground Pi2 pulsations, *J. Geophys. Res.*, *108*(A7), 1275, doi:10.1029/2002JA009340.

Kepko, L., and M. Kivelson (1999), Generation of Pi2 pulsations by bursty bulk flows, *J. Geophys. Res.*, *104*, 25,021–25,034, doi:10.1029/1999JA900361.

Mann, I. R., et al. (2008), The upgraded CARISMA magnetometer array in the THEMIS era, *Space Sci. Rev.*, *141*, 413–451, doi:10.1007/s11214-008-9457-6.

McPherron, R. L., C. W. Arthur, M. D. Bossen, and C. T. Russell (1973), Micropulsation substorm at synchronous orbit ATS-1 observations of ULF waves, *Eos Trans. AGU*, *54*, 420.

Menk, F. W., D. Orr, M. A. Clilverd, A. J. Smith, C. L. Waters, and B. J. Fraser (1999), Monitoring spatial and temporal variations in the dayside plasmasphere using geomagnetic field line resonances, *J. Geophys. Res.*, *104*, 19,955–19,970.

Milling, D. K., I. J. Rae, I. R. Mann, K. R. Murphy, A. Kale, C. T. Russell, V. Angelopoulos, and S. Mende (2008), Ionospheric localisation and expansion of long-period Pi1 pulsations at substorm onset, *Geophys. Res. Lett.*, *35*, L17S20, doi:10.1029/2008GL033672.

Murphy, K. R., I. J. Rae, I. R. Mann, D. K. Milling, C. E. J. Watt, L. Ozeke, H. U. Frey, V. Angelopoulos, and C. T. Russell (2009), Wavelet-based ULF wave diagnosis of substorm expansion phase onset, *J. Geophys. Res.*, *114*, A00C16, doi:10.1029/2008JA013548.

Murphy, K. R., I. J. Rae, I. R. Mann, A. P. Walsh, D. K. Milling, and A. Kale (2011), The dependence of Pi2 waveforms on periodic velocity enhancements within bursty bulk flows, *Ann. Geophys.*, *29*, 493–509, doi:10.5194/angeo-29-493-2011.

Murphy, K. R., I. R. Mann, I. J. Rae, C. Waters, B. Anderson, D. K. Milling, H. J. Singer, H. Korth (2012), Reduction in field-aligned currents preceding and local to auroral substorm onset, *Geophys. Res. Lett.*, *39*, L15106, doi:10.1029/2012GL052798.

Nishimura, Y., L. R. Lyons, T. Kikuchi, V. Angelopoulos, E. Donovan, S. Mende, P. J. Chi, and T. Nagatsuma (2012), Formation of substorm Pi2: A coherent response to auroral streamers and currents, *J. Geophys. Res.*, *117*, A09218, doi:10.1029/2012JA017889.

Nose, M., T. Iyemori, M. Takeda, T. Kamei, D. K. Milling, D. Orr, H. J. Singer, E. W. Worthington, and N. Sumitomo (1998), Automated detection of Pi 2 pulsations using wavelet analysis: 1. Method and an application for substorm monitoring, *Earth Planets Space*, *50*, 773–783.

Olson, J. V. (1999), Pi2 pulsations and substorm onsets: A review, *J. Geophys. Res.*, *104*, 17499–17520.

Peticolas, L. M., et al. (2008), The Time History of Events and Macroscale Interactions during Substorms (THEMIS) Education and Outreach (E/PO) Program, *Space Sci. Rev.*, *141*, 557–583.

Plaschke, F., K.-H. Glassmeier, O. D. Constantinescu, I. R. Mann, D. K. Milling, U. Motschmann, and I. J. Rae (2008), Statistical analysis of ground based magnetic field measurements with the field line resonance detector, *Ann. Geophys.*, *26*, 3477–3489.

Rae, I. J., I. R. Mann, D. K. Milling, Z. C. Dent, and A. Kale (2007), Pi2 pulsations: Field line resonances of a driven response?, in *Proceedings of the Eighth International Conference on Substorms*, edited by M. Syrjäsuo and E. Donovan, pp. 253-258, Univ. of Calgary, Alberta, Canada.

Rae, I. J., et al. (2009), Timing and localization of ionospheric signatures associated with substorm expansion phase onset, *J. Geophys. Res.*, *114*, A00C09, doi:10.1029/2008JA013559.

Rae, I. J., C. E. J. Watt, K. R. Murphy, H. U. Frey, L. G. Ozeke, D. K. Milling, and I. R. Mann (2012), The correlation of ULF waves and auroral intensity before, during and after substorm expansion phase onset, *J. Geophys. Res.*, *117*, A08213, doi:10.1029/2012JA017534.

Rostoker, G., J. C. Armstrong, and A. J. Zmuda (1975), Field-aligned current flow associated with intrusion of the substorm-intensified westward electrojet into the evening sector, *J. Geophys. Res.*, *80*, 3571–3579, doi:10.1029/JA080i025p03571.

Russell, C. T., P. J. Chi, D. J. Dearborn, Y. S. Ge, B. Kuo-Tiong, J. D. Means, D. R. Pierce, K. M. Rowe, and R. C. Snare (2008), THEMIS ground-based magnetometers, *Space Sci. Rev.*, *141*, 389–412.

Samson, J., and J. Olson (1980), Some comments on the descriptions of the polarization states of waves, *Geophys. J. R. Astron. Soc.*, *61*, 115–129.

Takahashi, K., et al. (1988), AMPTE/CCE observations of substorm-associated standing Alfven waves in the midnight sector, *Geophys. Res. Lett.*, *15*, 1287.

Zesta, E., L. R. Lyons, and E. Donovan (2000), The auroral signature of Earthward flow burst observed in the Magnetotail, *Geophys. Res. Lett.*, *27*, 3241.